MOLECULAR AND CELLULAR BIOLOGY, Jan. 1992, p. 10–21
0270-7306/92/010010-12$02.00/0

Vol. 12, No. 1

Proviral Rearrangements and Overexpression of a New Cellular Gene (*nov*) in Myeloblastosis-Associated Virus Type 1-Induced Nephroblastomas

V. JOLIOT,[1]† C. MARTINERIE,[1] G. DAMBRINE,[2] G. PLASSIART,[3] M. BRISAC,[1] J. CROCHET,[1] AND B. PERBAL[1,4]*

Laboratoire d'Oncologie Virale et Moléculaire, Batiment 110, Institut Curie, Centre Universitaire, 91405 Orsay Cedex,[1] Institut National de la Recherche Agronomique, Nouzilly,[2] Ecole Vétérinaire, Nantes,[3] and Université Paris VII, Paris,[4] France

Received 20 March 1991/Accepted 30 September 1991

Histological and anatomopathological studies performed on 152 independent myeloblastosis-associated virus type 1 (MAV1)-induced nephroblastomas allowed us to precisely define the chronology of tumor development in chickens. Three tumors representing increasing developmental stages were used to construct genomic libraries and to study both the state of proviral genomes and the sites of MAV1 integration in genomic DNA. We established that increasing levels of proviral rearrangement, eventually leading to the elimination of infectious MAV genomes, were associated with tumor progression and that 22 individual tumors, representative of different developmental stages, did not contain any common MAV1 integration site. Cloning of cellular fragments flanking the MAV1-related proviruses in tumor DNA showed that each one of eight nephroblastomas tested expressed a high level of an as yet unidentified cellular gene (*nov*) whose transcription is normally arrested in adult kidney cells. Cloning of the normal *nov* gene established that in one tumor, fused long terminal repeat-truncated *nov* mRNA species were expressed, indicating that at least in that case, the high level of *nov* expression was under the control of the MAV long terminal repeat promoter. The normal *nov* gene encodes a putative 32-kDa secreted polypeptide, which is a member of a new family of proteins likely to be involved in cell growth regulation. We also showed that the expression of an amino-terminal-truncated *nov* product in chicken embryo fibroblasts was sufficient to induce their transformation.

The avian nephroblastoma induced by myeloblastosis-associated virus (MAV) is generally considered a good model for the human Wilms' tumor because of their histological similarities (i.e., embryonic tissues consisting of a heterogeneous mixture of immature and differentiated renal elements) (18, 23). It is now well established that nephroblastoma development in humans is associated with deletion of at least one of two distinct genetic loci assigned to chromosome 11: 11p13 (11, 27, 33, 40), 11p15 (26, 37), and alteration of a locus outside of 11p (16, 21, 43). There is also a growing body of evidence to suggest that recessive alleles at these loci are involved in tumorigenesis. Recently, one of the candidate Wilms' tumor genes, located at the chromosome 11p13 locus within the WAGR complex, was reported to encode a potential zinc finger protein (7, 13).

We believe that studying MAV-induced nephroblastoma may lead to the characterization of molecular events associated with tumor development which might not be directly accessible in the human system. MAV is a replication-competent retrovirus responsible for the induction of nephroblastoma, osteogenic osteoblastoma (osteopetrosis), and, less frequently, lymphoid leukemia and sarcoma in chickens (48). On the basis of differences in their pathogenicity, two strains of MAV2 were identified as inducing preferentially osteopetrosis [MAV2(O)] or nephroblastoma [MAV2(N)], although plaque-purified MAV2(O) and MAV2(N) still induced 20% nephroblastomas and 30% osteopetrosis, respectively (48, 53). T_1-resistant oligonucleotide maps established for these two viral strains confirmed that they were genetically distinct (54), but the molecular basis of tumor induction by MAV remains to be elucidated. On one hand, studies of nephroblastoma induced with plaque-purified MAV2(O) did not detect proviral insertion in the vicinity of known proto-oncogenes (5); on the other hand, a provirally activated c-Ha-*ras* was revealed in one case of MAV2(N)-induced nephroblastoma (55). Insertional mutation and transduction of the c-*fos* proto-oncogene have also been reported in avian leukosis virus-induced nephroblastomas (8, 31).

We have previously reported the isolation of an infectious MAV1 proviral clone (35) and shown that the corresponding genetically pure MAV1 strain induced specifically nephroblastomas when injected into day-old chicks (49). This system therefore represented a unique tool with which to study the molecular events involved in the genesis of MAV-induced nephroblastoma in chickens and to determine whether the avian and human tumors might share common pathways of induction.

After a preliminary characterization of the state of proviral DNA in tumor cells, we had reported evidence suggesting that nephroblastomas are polyclonal tumors (49). We could show, in addition, that the MAV1-induced nephroblastomas contained a number of rearranged proviral genomes which increased in number with the development of the tumors (49). To understand the relationship that might exist between proviral rearrangements and tumor induction or progression, we analyzed the proviral content of several independently induced nephroblastomas and characterized the MAV1 integration sites in tumor DNA. The results reported below show that the rearrangements of proviral sequences, which increase with tumor progression, result in the elimination of

* Corresponding author.
† Formerly V. Maloisel.

intact MAV1 proviruses and give rise to MAV1-related structures bearing only one long terminal repeat (LTR). Also, all of the tumors that we have tested express a high level of an as yet unidentified gene (*nov*) which belongs to a new family of immediate-early genes likely to play a role in cell growth regulation. We report for the first time that overexpression of such a gene is associated with tumorigenesis and that expression of a truncated version of *nov* in chicken embryonic fibroblasts (CEF) is sufficient to induce the transformation of CEF in vitro.

MATERIALS AND METHODS

Virus and chicken strains. The MAV1 strain used in this study was propagated from CEF transfected with the DNA of a λ 311411 MAV1 proviral clone (35) under previously described conditions (49).

Chickens were from the C/E Brown Leghorn Edinburgh strain (gs^+ chf^+ V^-) from Station de Pathologie Aviaire et de Parasitologie, Institut National de la Recherche Agronomique, Nouzilly, France. Day-old chicks were inoculated as previously described (49).

Histological analysis. Every fifth day, following inoculation, five birds were sacrificed and necropsied. Kidneys from two control and from three infected chickens were fixed in toto by immersion in Holland Bovin's fixative or neutral formalin.

For each animal, four kidney samples (i.e., one sample for each rostral and caudal lobe of the left and right kidneys) were then embedded in paraffin. Sections (5 to 6 μm thick) were routinely stained with hemalum-eosis-saffron.

Periodic acid-Schiff, Masson's trichrome (9), and Jowe's silver methenamine (24) staining were also performed when necessary.

Molecular cloning. Procedures for nucleic acid purification, Southern and Northern (RNA) blotting, and standard cloning protocols were described previously (34). Dichloromethane was used instead of chloroform for nucleic acid purification (29). Recombinant lambda DNA was prepared as described previously (15).

Viral probes. The HI91, EBG, BGE, and EXE probes used for screening genomic libraries and mapping restriction sites of recombinant clones were previously described (35, 50). The MAV U3-specific probe (HO) is a 160-nucleotide *oxa*NI-*Hin*dIII DNA fragment derived from the MAV1 U3 LTR sequences and subcloned in pUC. This probe does not cross-react with other retroviral U3 sequences (55).

Preparation of genomic libraries. Genomic libraries of tumor DNA (tumors 501D, 501, and 725, described in reference 49) were constructed in lambda EMBL4. High-molecular-weight DNA (150 μg) purified from each tumor was partially digested with *Eco*RI and fractionated by centrifugation through a 10 to 40% sucrose gradient. DNA samples (1.5 μg) ranging in size from 15 to 20 kb were ligated to 3 μg of *Eco*RI-digested lambda EMBL4 DNA and used to infect *Escherichia coli* P2 after in vitro packaging (28). A total of 4×10^5 to 5×10^5 recombinant clones from each library screened by hybridization with ^{32}P-labeled nick-translated U3-specific probe under stringent conditions (34) gave rise to 29 independent clones whose structures are described in Results.

Genomic probes. Genomic DNA fragments free of repetitive sequences and containing the cellular sequences flanking proviral genomes in tumor DNA were purified and subcloned in pUC18, pUC19, or pBR322 to generate the probes represented in Fig. 2.

Isolation of *nov* cDNA. A 25-ng sample of cDNA [corresponding to 13-day-old CEF poly(A) RNA] was ligated with 1 μg of lambda gt10 arms to prepare a normal chicken fibroblast cDNA library, using an Amersham kit. Following screening with the HX1024 probe, seven clones were purified. The longest insert (1.9 kb) was purified according to the Geneclean method (Bio 101) and subcloned at the *Kpn*I site of Bluescript KS+ (Stratagene) to generate the pC1K clone.

Nucleotide sequencing. Sequencing was performed by the dideoxy-chain termination method (42) in the presence of [α-^{35}S]dATP and either T7 polymerase (Pharmacia) or Sequenase (U.S. Biochemical) under the conditions described by the manufacturers. Templates were obtained from M13mp18 and M13mp19 recombinant clones. Sequencing primers were purchased from New England Biolabs. GC compressions were resolved by using deoxyinosine (U.S. Biochemical). Sequence data treatments were performed by using the computer facilities at CITI2 in Paris.

cDNA polymerase chain reaction (PCR) amplification of tumor RNA. One microgram of poly(A) RNA purified from tumor 725 was used to direct cDNA synthesis in the presence of 1.6 μg of oligo(dT) under the conditions recommended in the Amersham kit. Following RNA hydrolysis at 50°C for 30 min in the presence of 300 mM NaOH and neutralization with 214 mM HCl–70 mM Tris-HCl (pH 7.5), the cDNA was purified from nucleotides, oligo(dT), and salts by two successive centrifugations through Centricon C-100 microconcentrators (Amicon).

The two amplimers used for PCR amplification were synthesized on an Applied Biosystems synthesizer. They are (i) specific for the U5 region of the MAV1 LTR (5′-ACCTC TCACCACATTGGTGT-3′) and (ii) complementary to the 3′ and 5′ boundaries of *nov* exons 2 and 3, respectively (5′-TGTCTGTATGCAGCCATAGC-3′).

PCR amplification was performed in the presence of 1 ng of cDNA and 40 pmol of each primer under the conditions initially recommended by Cetus (200 mM each deoxynucleoside triphosphate, 5% [vol/vol] dimethyl sulfoxide, and 2.5 U of *Taq* polymerase in a total volume of 100 μl). Thirty cycles (2 min of denaturation at 94°C, 30 s of annealing at 55°C, and a 1-min extension at 72°C) followed by a 6-min final extension at 72°C were carried out in a Perkin-Elmer Cetus DNA thermocycler. The PCR products to be sequenced were blunt ended in the presence of Pol1K (New England Biolabs), phosphorylated in the presence of polynucleotide kinase (New England Biolabs), and subcloned at the *Sma*I site of M13mp19. Recombinant clones containing the relevant sequences were isolated following hybridization with ^{32}P-labeled oligonucleotidic probes (5′-CTTCAGCTT CATTCAGGTGT-3′ and 5′-ACACCTGAATGAAGCTGA AG-3′) specific for the MAV U5 sequences which were expected to be coamplified.

Construction of pRSV recombinants and transfection. A *Bam*HI-*Hin*dIII fragment containing *nov* sequences (nucleotides 1 to 1452) and five nucleotides of polylinker was cloned at the corresponding restriction sites in the CLA12 adaptor plasmid (22). The truncated *nov* sequences represented in tumor 725 which are delineated by an *Ava*I site (nucleotide 289) and a *Hin*dIII site (nucleotide 1452) were cloned at the *Sma*I site of plasmid CLA12 following fill-in with Pol1K. These inserts were subcloned at the *Cla*I site of the RCAS nondefective Rous sarcoma virus (RSV)-derived proviral vector (22). The *Cla*I site is located 3′ to a splice acceptor, which allows the synthesis of a subgenomic *nov* mRNA whose translation starts at a *nov*-specific initiation codon. Clones pRSV 172 and pRSV 173 contain the entire

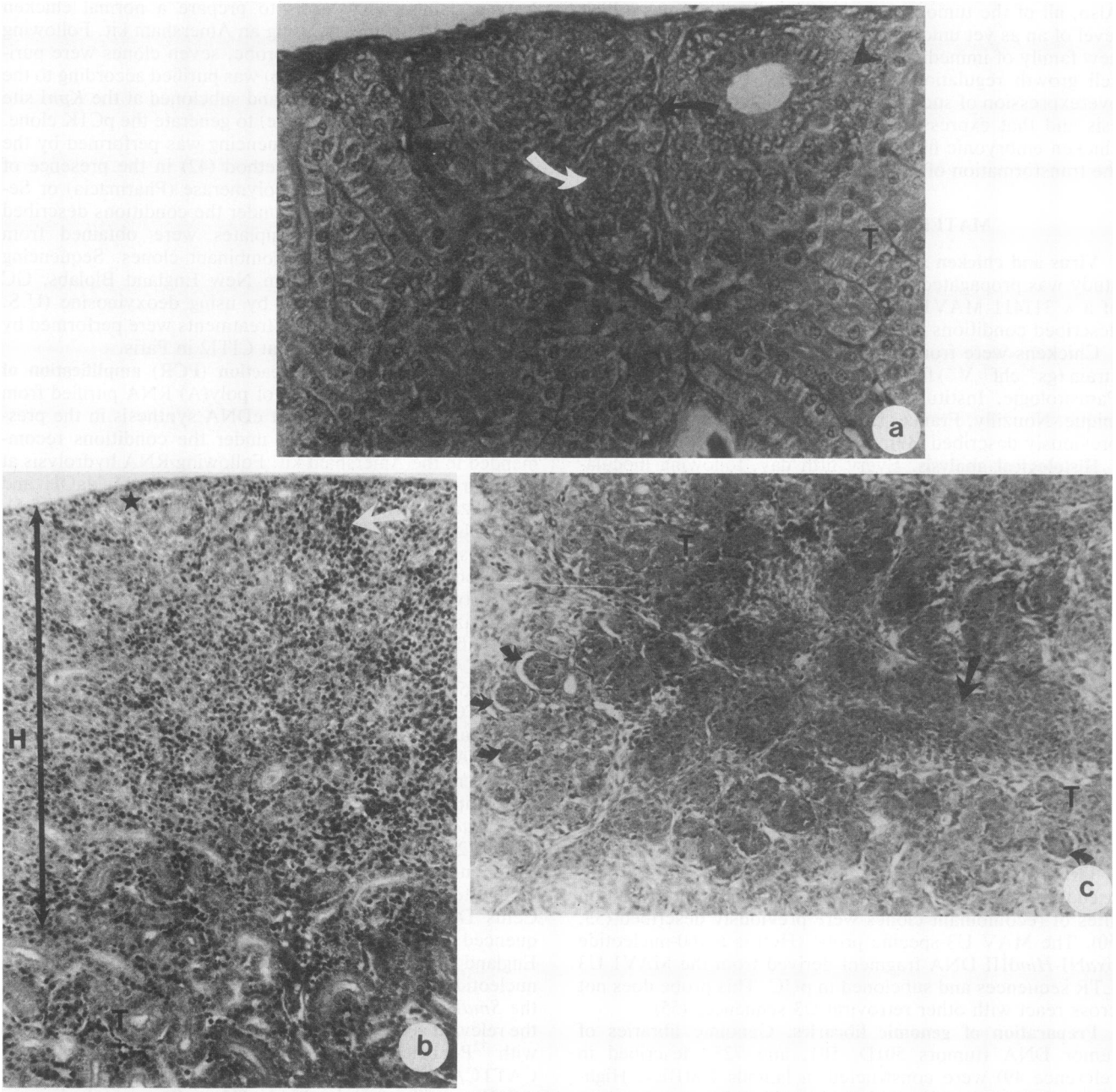

FIG. 1. Histological and anatomical studies of nephroblastoma appearance and development. (a) Normal kidney, control chicken, subcapsular embryonic rest. Seen is a nest of nephrogenic cells (arrowheads), with an island of primitive epithelial differentiation (white arrow) from which tubules are differentiating (curved arrow). Also seen are well-differentiated urinary tubules (T). Magnification, ×246. (b) Pretumoral lesion, infected chicken. Seen are a hyperplastic lesion (H) with foci of blastema cells (star) and numerous poorly differentiated urinary tubes (arrow); diffuse inflammatory infiltration is composed mainly of lymphocytes and plasma cells. The underlying renal tissue shows well-differentiated tubules (T). Magnification, ×66. (c) Nephroblastoma. The tumoral tissue is composed of a mixture of cords of nephrogenic cells (straight arrows), urinary tubules (T), and abortive glomerules (curved arrows) enclosed in a loose, clear connective tissue. Magnification, ×123. (d) Nephroblastoma. Rare tubular structures (arrow) are surrounded by undifferentiated cells in an irregular pattern. A large amount of cartilage is present (star). Some epithelial structures undergo epidermoid metaplasia (curved arrow). Magnification, ×41. (e) Mesangioproliferative glomerulonephritis. Glomeruli are highly hypertrophied. The floculus is invaded with mononuclear cells (white arrowhead). Glomerular capillaries are barely visible. Urinary space is often reduced (black arrow); adherences link Bowman's capsule to flocculus (white arrow). (×200). (f) Histogram of the appearance of tumor lesions in 152 chickens after MAV1 inoculation. Vertical axis, percentage of chickens presenting no macroscopic lesion (□), renal hypertrophy (▨), or characteristic nephroblastomas (diameter, >1 cm) emerging clearly from renal lobes (■). Horizontal axis, days postinoculation. The age of each tumor analyzed is represented by arrows at the bottom.

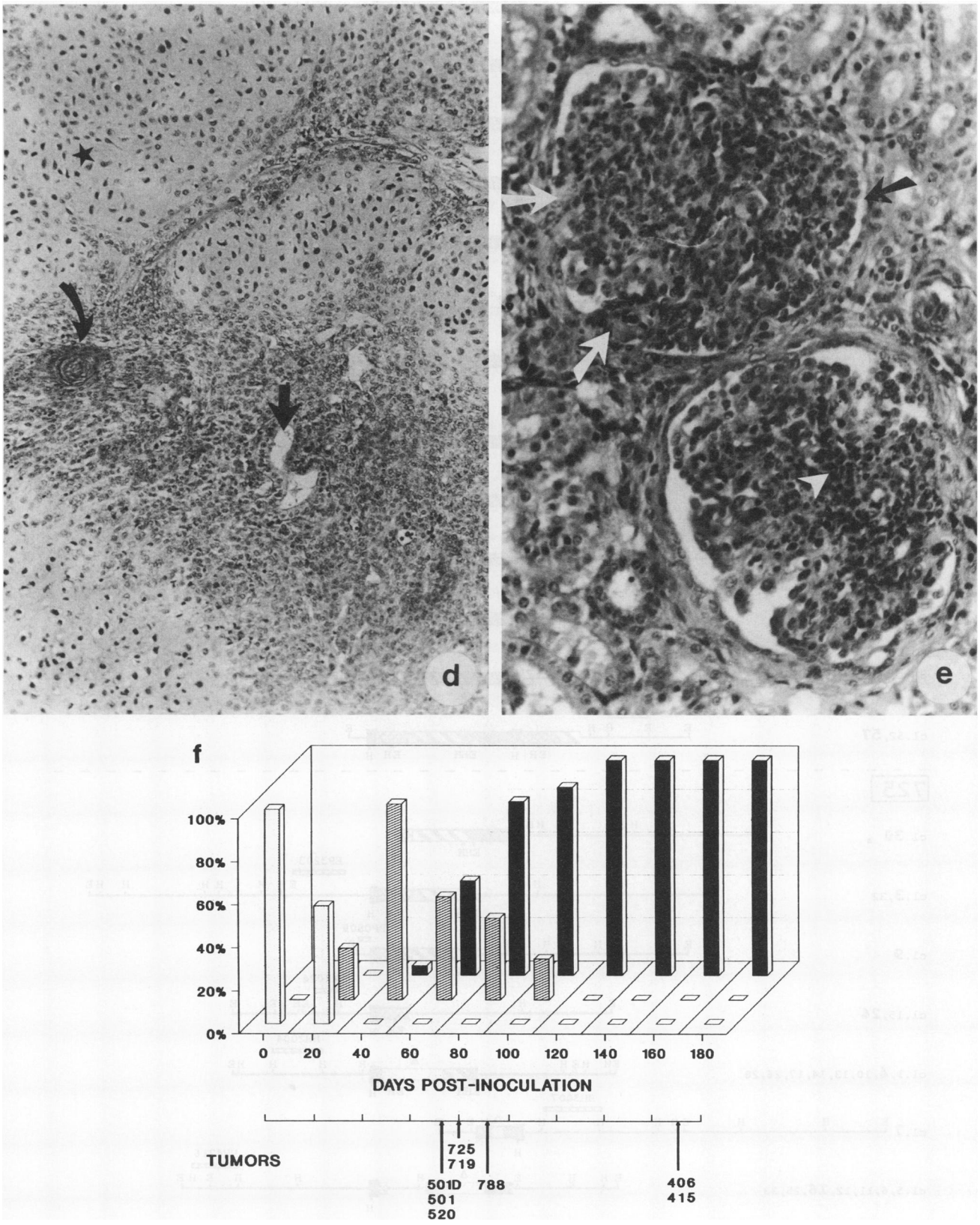

FIG. 1—*Continued.*

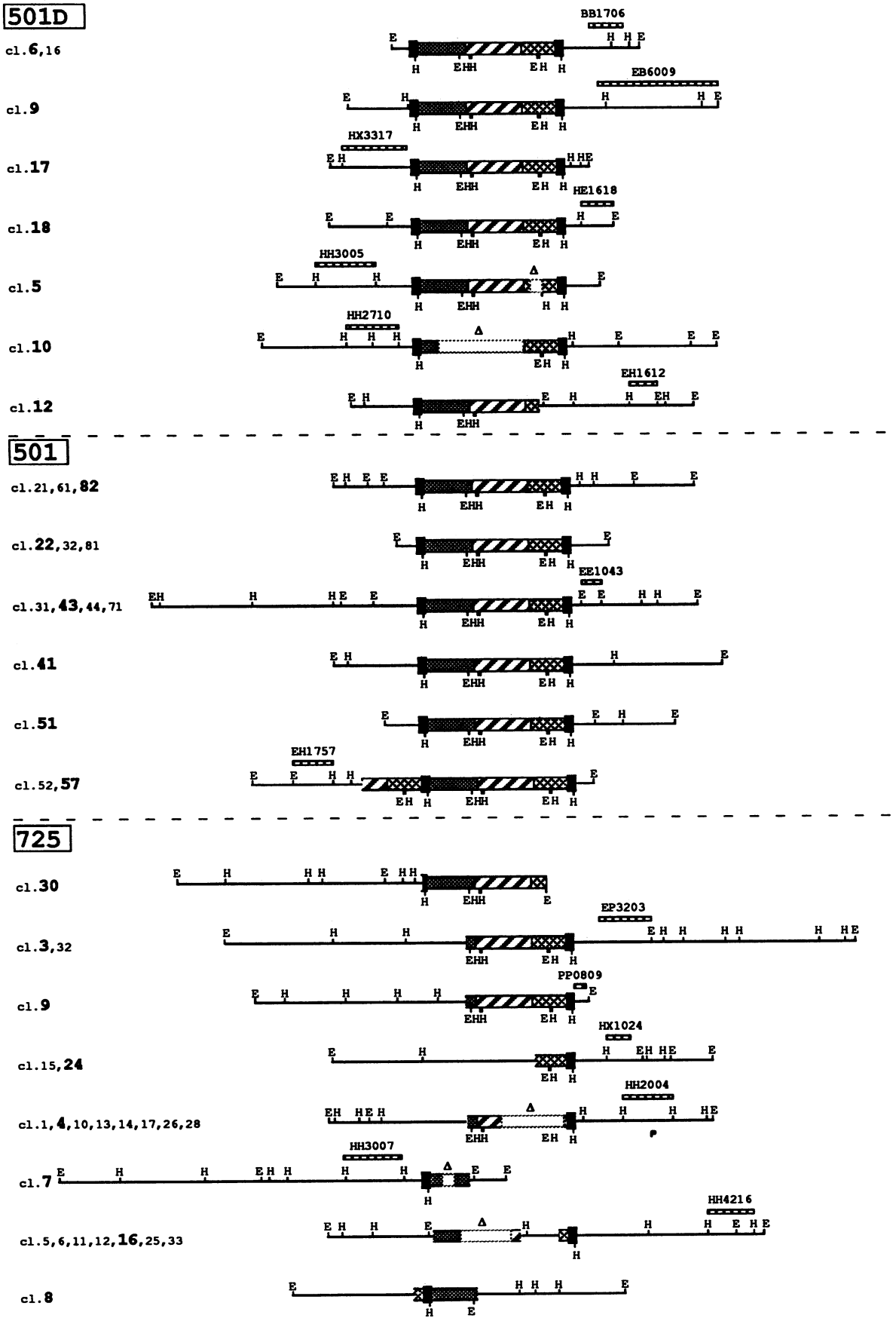
501D
cl.6,16
BB1706
cl.9
EB6009
cl.17
HX3317
cl.18
HE1618
cl.5
HH3005
cl.10
HH2710
cl.12
EH1612
501
cl.21,61,82
cl.22,32,81
cl.31,43,44,71
EE1043
cl.41
cl.51
cl.52,57
EH1757
725
cl.30
cl.3,32
EP3203
cl.9
PP0809
cl.15,24
HX1024
cl.1,4,10,13,14,17,26,28
HH2004
cl.7
HH3007
cl.5,6,11,12,16,25,33
HH4216
cl.8

FIG. 2. Organization of MAV1 proviruses and cellular flanking sequences in nephroblastomas 501D, 501, and 725. Twenty-nine independent clones were isolated after screening of the genomic libraries with a probe specific for U3 MAV sequences (see Materials and Methods). 501D and 501 did not reveal common features even though these tumors were derived from the same animal, indicating that they were primary tumors and not metastases. The largest restriction maps are a compilation of several overlapping clones. Symbols: ■, LTR; ■, *gag*; ▨, *pol*; ▩, *env*; △, viral regions deleted. The cellular restriction fragments used as probes are indicated above the maps. E, *Eco*RI; H, *Hin*dIII; cl., clone.

nov sequences, and clones pRSV 171 and pRSV 170 contain the truncated *nov* sequences, both inserts being in either the correct orientation or the wrong orientation, respectively.

Ten micrograms of each recombinant plasmid DNA was used to transfect Brown Leghorn CEF under the conditions previously described (50). Growth without anchorage was assayed as described previously (50) in the presence of 10 μg of high-molecular-weight dextran sulfate (Pharmacia) per ml.

Nucleotide sequence accession number. The sequence reported has been deposited in the GenBank/EMBL data bases under accession number X59284 CHICKEN NOV CDNA.

RESULTS

Tumor development: anatomical and histological definition of two different stages. Histological studies of MAV1-infected kidneys revealed two successive stages in tumor development (Fig. 1). From days 11 to 53 postinfection, a hyperplasia of the metanephric renal blastema caused hypertrophy. The hyperplastic tissue was infiltrated with inflammatory cells composed mainly of lymphocytes and plasma cells. Lymphoid follicles were also frequently observed. We call this the pretumoral period (Fig. 1b). MAV1-specific sequences could be detected by PCR analysis in kidneys as well as in other tissues from day 4 postinoculation throughout the pretumoral stage (unpublished observations).

At and after this hypertrophic stage, mild irregularities could be observed in the vicinity of the renal blastema: urinary tubules were more convoluted, tubular epithelial cells became more basophilic, and glomeruli were more numerous than in kidneys of control animals. Regression of the hyperplasia was correlated with the emergence of typical nephroblastomas (>1 cm) on renal lobes from day 53 onwards. This corresponded to the beginning of the tumor stage. Multiple renal tumors of variable size could often be found in the same animal. At this stage, the tumoral tissue was composed of epithelial and connective derivatives, stroma, and undifferentiated blastema cells, often associated with aberrantly organized abortive tubules and glomeruli (Fig. 1c).

In agreement with previous reports (3, 18, 23), the histological aspect of the larger tumors (>6 cm), such as tumor 725, showed a more varied pattern. Beneath the components described in early tumors, the more developed tumors contained variable amounts of cartilaginous and osseous tissues, and in most tumors, inflammatory infiltration could not be detected (Fig. 1d). Glomerular lesions, similar to mammalian proliferative glomerulonephritic lesions (46), became particularly obvious 53 days postinoculation (Fig. 1e). Our cytological observations, in accordance with previous findings (17, 19), revealed that nephroblastomas in chickens are nonmetastatic, suggesting that they may have a multicentric origin.

Progression in tumor differentiation correlates with increasing rearrangements of proviral sequences and loss of one LTR. Genomic libraries were constructed with tumors 501D, 501, and 725, which are representative of different developmental stages and differentiation states (49). All of the viral/cellular junctions of the constructed MAV-specific clones corresponded to the clonal junction fragments previously identified by Southern blotting in these tumors (49), indicating that the MAV1 proviral clones originated from tumor cells.

Most proviruses from tumors 501D and 501 appear to represent full-length MAV1 genomes with normal restriction maps. We have ascertained by interference assays of transfected CEF (51) that the full-length MAV provirus of clone 43 (tumor 501) yielded infectious progeny. Also, probe EE1043, which contained flanking cellular sequences, detected clonal fragments in the DNA from tumor 501 (data not shown). These observations demonstrated that intact infectious proviruses were present in the genome of tumor cells.

Two MAV1 proviruses in tumor 501D (clones 5 and 10) sustained internal deletions, while another one lost 3′-proximal sequences, including the LTR (clone 12). Only one clone from tumor 501 (clone 57) contained a rearranged provirus lacking 5′-proximal sequences (Fig. 2). This truncated provirus shares its 3′ LTR sequences with a normal MAV1 provirus, suggesting that tandem integration of MAV proviruses occurred in the target cells.

In tumor 725, seven of eight clones contained MAV proviruses devoid of one LTR and harboring extensive rearrangements of internal sequences. In the eighth clone (clone 30), the partially cloned MAV1 was also altered, since nucleotide sequencing of the 5′ LTR revealed a deletion of 30 bp at the 5′ boundary of the U3 domain (data not shown).

The structures of the rearranged proviruses from tumor 725 suggested that the proviruses had undergone additional (and possibly successive) rounds of alterations and that the neoplastic cells in tumor 725 did not contain any full-length MAV provirus. Therefore, it is likely that proviral rearrangements were correlated with tumor progression.

Different nephroblastomas do not contain a common proviral integration site. Southern hybridization performed with probes containing cellular sequences flanking the proviruses cloned from tumors 501D, 501, and 725 (Fig. 2) established that rearrangement of cellular sequences occurred only in the vicinity, and after deletion, of the proviral LTR (data not shown). Cellular sequences flanking intact LTRs were therefore likely to represent the sites of proviral integration in host DNA.

All of the probes corresponding to the original MAV1 integration sites in tumor 725 (Fig. 2) were hybridized to the DNAs of 22 other independently generated nephroblastomas. Except in one case, the DNA fragments identified were found to be in germ line configuration in all of the tumors examined (data not shown). Only probe PP0809 detected a DNA rearrangement in a single other tumor. These observations indicated that the domains of proviral integration in tumor 725 were not targeted for proviral integration in the other tumors examined (at least within a range of 14 kb of sequences).

Characterization of a new cellular gene (*nov*) whose expression is upregulated in nephroblastomas. Northern blot analysis of RNA isolated from normal kidneys, CEF, and nephroblastomas was performed with the cellular probes derived from tumor 725 (Fig. 2). Only one of these probes (HX1024) detected in normal CEF a mRNA species (2.2 kb) whose expression was altered in all the nephroblastomas tested (see below). The corresponding gene has been designated *nov* (for nephroblastoma-overexpressed gene).

A shorter *nov* mRNA species (2.0 kb) was found to be specifically overexpressed in tumor 725 (Fig. 3A). A 5.2-kb mRNA species was also expressed, but at a much lower level. Two probes (HX0724 and EE2424) derived from cellular sequences upstream and downstream, respectively, of the sequences represented in HX1024 (Fig. 3A) also detected both mRNAs (data not shown). The 5.2-kb mRNA, which was the only one detected by probe HX0924, presumably contained sequences spliced out in the 2.0-kb mRNA species (Fig. 3A).

The use of a *nov* cDNA (see below) as a probe established that a 2.2-kb *nov* mRNA was overexpressed in four highly differentiated nephroblastomas (719, 788, 406, and 415) and to a lesser extent in tumors 501D, 501, and 520, which represented earlier tumoral stages (Fig. 3B).

In the day 18 embryonic kidney, the *nov* mRNA species (2.2 kb) was easily detected, whereas after hatching, expression of the 2.2-kb mRNA was reduced to a barely detectable level (Fig. 3B). These observations suggest that the expression of *nov* is related to the differentiation state of renal tissues, since it is repressed in the normal adult kidney and reexpressed at a high level in all MAV1-induced nephroblastomas tested. The levels of *nov* expression in the pretumoral MAV1-infected kidneys (days 4 to 46) and in the kidney of uninfected control animals were similar (data not shown), indicating that MAV1 multiplication was not sufficient to induce overexpression of *nov*.

Hybridization experiments performed with various fetal chicken tissues demonstrated that the 2.2-kb *nov* mRNA was expressed predominantly in the brain and the heart and at a lower level in muscle and intestine (Fig. 3C). It was not expressed in lung, liver, and yolk sac. In adult chicken tissues, *nov* was highly expressed in lung and less so in brain and spleen. It was not detected in muscle, liver, and heart (Fig. 3C). In addition, *nov* transcripts were not expressed in two avian tumorigenic hematopoietic cell lines (BM2 and MSB1), indicating that the overexpression of *nov* in nephroblastomas was not simply the result of virus-induced cell proliferation (Fig. 3).

Synthesis of chimeric MAV-*nov* RNA by a rearranged proviral genome in nephroblastoma 725. Nucleotide sequencing of a *nov* cDNA clone and of the corresponding genomic fragments demonstrated that *nov* was composed of at least five exons (Fig. 4B) spanning about 10 kb of DNA and that in the genome of tumor 725, an altered MAV1 proviral genome was integrated in the second exon of *nov* (Fig. 4C). PCR experiments showed that the 2.0-kb mRNA overexpressed in nephroblastoma 725 was a chimeric message containing both cellular and viral sequences. The viral nucleotide sequence upstream of the junction which occurs at position 201 (Fig. 4A) was identical to the 91 3′-proximal nucleotides of the MAV LTR U5 domain. The first putative ATG initiation codon (position 318) was in the cellular sequence and corresponded to an internal methionine codon in normal mRNA.

These results indicated that the 2.0-kb mRNA, whose transcription was probably initiated in the MAV LTR in nephroblastoma 725, represented a truncated version of the normal 2.2-kb message expressed in fibroblastic cells.

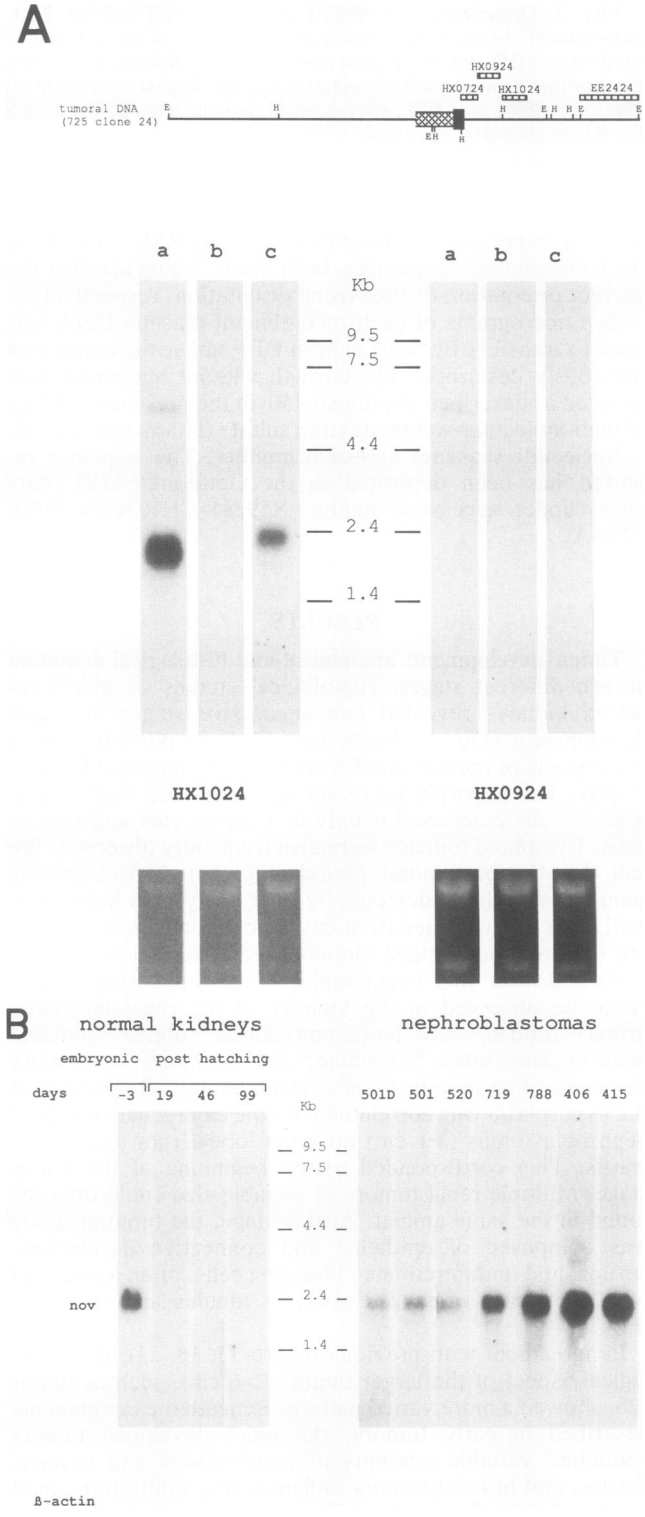

Sequence analysis of the *nov* cDNA clone. Figure 4A depicts the nucleotide sequence of the 1,975-bp *nov* cDNA clone. A 1.0-kb open reading frame encoding a putative protein of 32,300 Da was identified between nucleotides 24 and 1076. This open reading frame is followed by a 899-bp 3′ noncod-

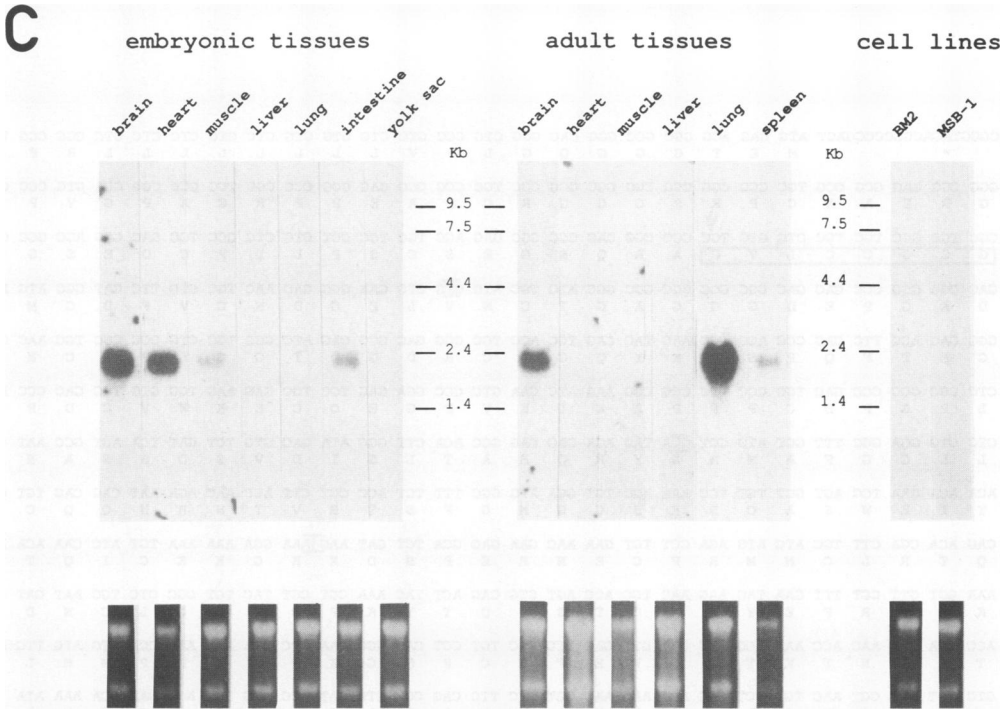

FIG. 3. Expression of *nov* in independently MAV1-induced nephroblastomas and in normal chicken tissues. (A) The cellular restriction fragments used as probes in Northern blotting analysis are indicated above the map of tumor DNA. Samples containing 10 μg of total RNA were hybridized with either probe HX1024 or probe HX0924. Lanes: a, tumor 725; b, normal adult kidney; c, normal CEF. (B) Total RNAs (10 μg) from normal chicken embryonic kidney, from normal chick kidney, and from several nephroblastomas were hybridized with a ^{32}P-labelled *nov* cDNA insert. (C) Total RNAs (10 μg) from various day 18 embryonic tissues (day −3), adult tissues, and tumoral avian cell lines (BM2 and MSB-1) were subjected to Northern transfer and hybridized with the ^{32}P-labelled *nov* cDNA insert. The Bethesda Research Laboratories RNA ladder was used for size markers. Amounts of RNA were normalized following ethidium bromide staining of rRNA for cell lines or tissue mRNA from different origins (A and C) or following hybridization with a β-actin probe (2) when mRNAs from the same tissue were tested (B).

ing sequence that contains two putative consensus polyadenylation signals (AATAAA at nucleotide positions 1914 and 1932).

The potential *nov* polypeptide contains a hydrophobic core characteristic of a signal peptide at its amino terminus (with a stretch of six leucines). The von Heijne weighted matrix method (52) predicts cleavage to occur between amino acids Val (position 24) and Ser (position 25). However, since the *nov* protein lacks other hydrophobic regions which are present in transmembrane proteins (10), it is likely to be secreted. The *nov* protein contains the consensus GCGCCXXC motif of insulinlike growth factor (IGF)-binding proteins (IGFBP) (1, 4, 6) and a total of 39 nonclustered cysteine residues. The 29 scattered proline residues prevent α-helix formation throughout much of the *nov* product. Proline is not present between amino acids 171 and 242, and a basic region can be recognized between residues 253 and 269. In tumor 725, the truncated *nov* product lacked both the signal peptide and the IGFBP consensus sequence.

The amino acid sequence of the *nov* protein shares an overall homology of approximately 50% with the expression products of a new family of genes, designated *CEF-10* (47), *CYR-61* (32), and *FISP-12* (41), which are thought to play a role in cell proliferation regulation. The invariant position of the 38 cysteine residues contained in these four proteins led us to recognize two highly conserved domains (residues 6 to 170 and 221 to 335 in *nov*) separated by a stretch of less conserved amino acids (Fig. 5). In all four proteins, the first domain contains the IGFBP consensus sequence (Fig. 5). However, these proteins are distinct from previously described IGFBP (25) and are likely to constitute a new family of secreted regulatory proteins.

Interestingly, these proteins exhibit different expression patterns, and the *nov* mRNA species are the only members of this family which do not contain the 3′-proximal TTATT TAT motif that confers instability to transcripts (45).

Biological properties of the *nov* products. To directly assess the oncogenic potential of the *nov* gene products, we have constructed RSV-derived replication-competent retroviral expression vectors harboring either the full-length *nov* gene or the subset of *nov* sequences expressed in tumor 725. Propagation of the recombinant viruses was obtained following transfection of CEF with purified DNAs, and the RSV-directed expression of *nov* in the infected cells was established by Northern blot analysis (data not shown).

CEF cultures infected with the truncated-*nov* recombinant (pRSV 171) gave rise to a significant number of dense foci of transformed cells (Fig. 6D) able to grow without anchorage, as revealed by their capacity to form large size colonies when seeded in soft agar. Secondary cultures derived from these isolated foci gave rise to dense foci of transformed cells and colonies in soft agar. In contrast, very few foci and no colonies were obtained in soft agar with CEF infected with the pRSV 170, pRSV 172, and pRSV 173 RSV recombinants carrying either the truncated or the intact *nov* gene cloned in both orientations (Fig. 6C, E, and F). Unexpectedly, the RSV-mediated expression of the normal *nov* gene

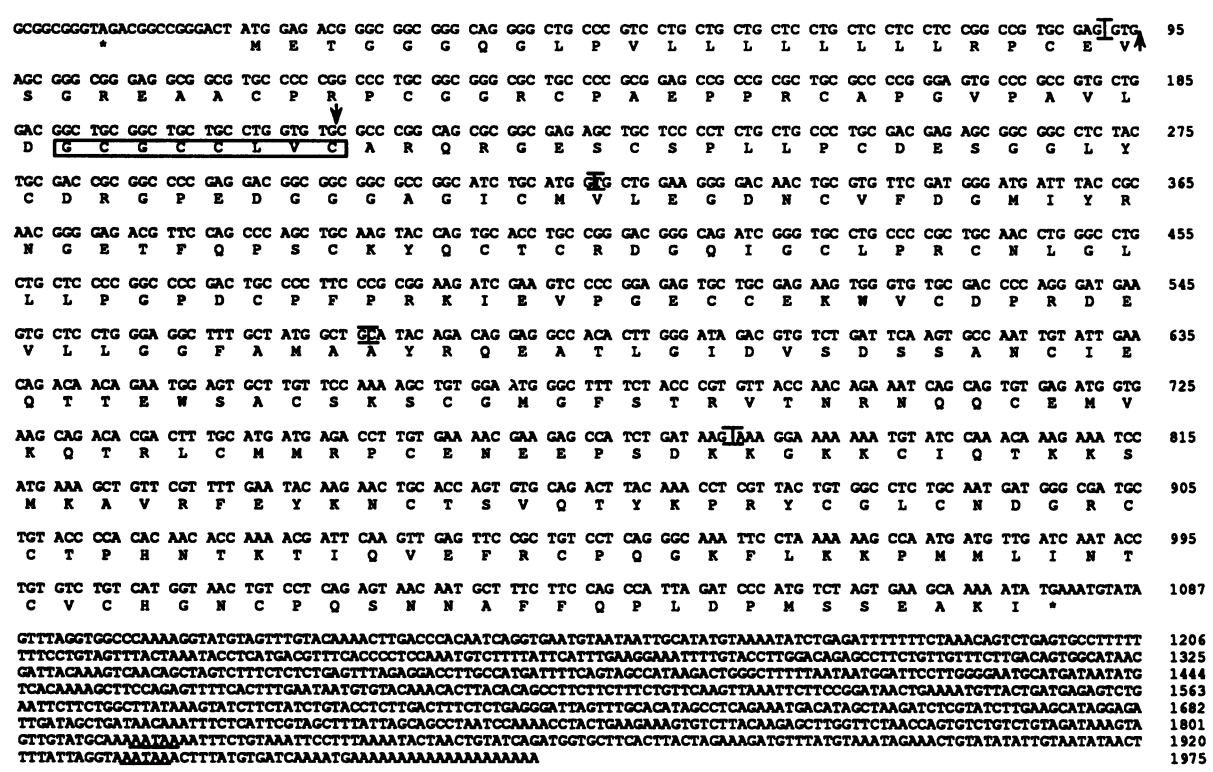

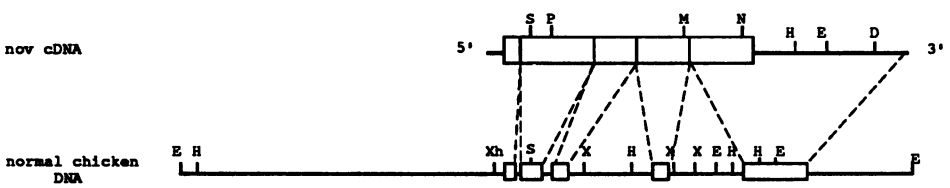

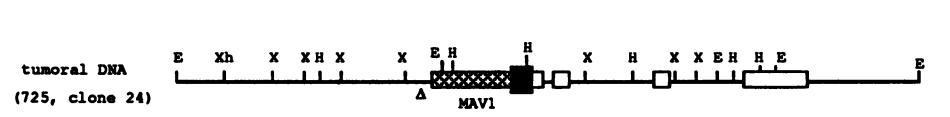

FIG. 4. Nucleotide sequence of the *nov* cDNA and deduced amino acid sequence and genomic organization of the normal and tumoral *nov* gene. (A) Sequences. The predicted amino acid sequence is shown below the corresponding nucleotide sequence. The consensus polyadenylation signals AATAAA are underlined. Stop codons are designated by an asterisk. Exons are delineated by brackets. The boxed amino acid sequence represents the IGFBP consensus (GCGCCLVC). The predicted peptide signal cleavage site is indicated by a vertical arrow between amino acids V and S at nucleotide position 95. The integration site of MAV provirus in the DNA of tumor 725 is indicated by the upper arrow between nucleotides TG and CG (position 211). (B) Restriction map of the longest *nov* cDNA clone isolated (top) and genomic map of normal chicken DNA. Empty boxes represent exonic sequences and coding regions. E, *Eco*RI; H, *Hin*dIII; X, *Xba*I; Xh, *Xho*I; S, *Sma*I; P, PvuII; M, *Mst*II; N, *Nde*I; D, *Dra*I. (C) Schematic representation of MAV1 sequences integrated in the *nov* locus of tumor 725. Symbols: ▭, *nov* exonic sequences; ▩, MAV env; ■, MAV LTR. E, *Eco*RI; H, *Hin*dIII; X, *Xba*I; Xh, *Xho*I.

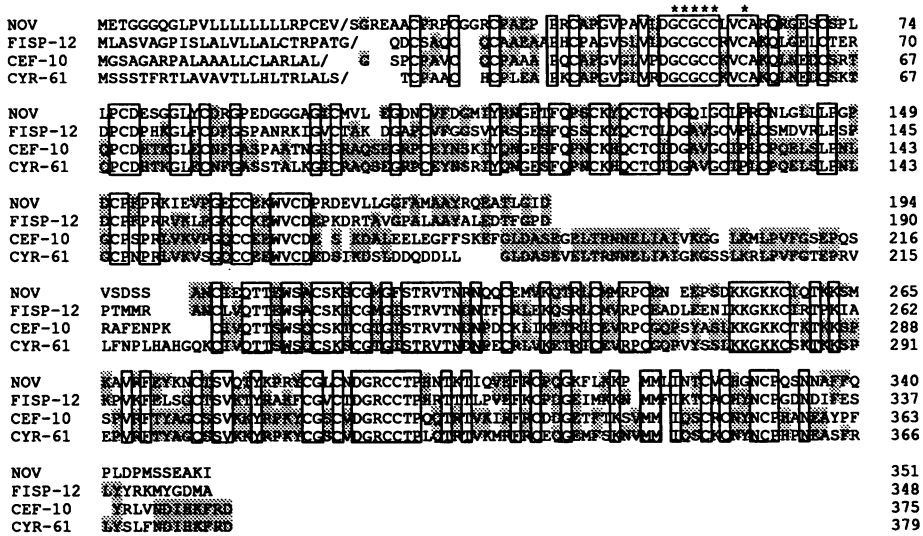

FIG. 5. Comparison of the deduced amino acid sequences for *nov*, *FISP-12*, *CYR-61*, and *CEF-10*. Sequences have been aligned to give maximal homology. *nov* shares 52% homology with *FISP*-12, 41% with *CYR-61*, and 42% with *CEF-10*. *CYR-61* is the mouse homolog of chicken *CEF-10* (32). The conserved residues in the sequences are boxed. Identical residues in two or three sequences are shaded. Stars indicate the IGFBP consensus motif (GCGCCXXC). Putative cleavage sites of the signal peptides are indicated.

in CEF resulted in a marked inhibitory effect on their growth capacity (Fig. 6E).

DISCUSSION

Understanding the molecular basis of nephroblastoma induction by MAV is of particular interest because (i) very little is known about the mechanism by which this nondefective retrovirus leads to oncogenic transformation and (ii) it is considered a good animal model for the human Wilms' tumor.

Our data indicate that tumor progression is correlated with a stepwise elimination of intact proviruses and the appearance of increasingly rearranged MAV1 proviral sequences. The final stage is exemplified by tumor 725, in which a complete provirus cannot be detected. Aside from the loss of one LTR, common viral rearrangements could not be identified in tumors from independent origins.

Alterations of the viral genome that result in the abrogation of viral expression might permit tumor cells to elude immune surveillance, as already suggested in the case of other nondefective transforming retroviruses (12, 14, 20, 38). Alternatively, these alterations might be required to generate LTR-derived structures which act as transcription activators and are responsible for growth stimulation or differentiation of the tumor cells.

In our search for possible specific integration sites in the genomic DNA of independent tumors, none of the probes derived from tumor 725 detected a common MAV1 integration site in 22 nephroblastomas tested.

All tumors expressed high levels of a new cellular gene (*nov*) sharing homologies with the *CYR-61* (32), *CEF-10* (47), and *FISP-12* (41) immediate-early genes.

PCR experiments revealed a fused viral/cellular message encoding a truncated *nov* gene product in tumor 725. The very high expression of this mRNA species probably results from its control by the viral LTR promoter. Downstream promotion of a proto-oncogene (c-Ha-*ras*) by the MAV LTR has been reported, but in only one case of MAV2(N)-induced nephroblastoma (55).

The present finding is unique because (i) the LTR-activated gene (*nov*) had not been detected previously, (ii) the expression of *nov* is normally repressed in the normal adult kidney, and (iii) *nov* is overexpressed (to a variable extent) in all of the nephroblastomas that we have tested.

Since the presence of viral sequences in the immediate vicinity (13 kb) of the *nov* gene could be demonstrated only in the case of tumor 725, the downstream promotion of *nov* did not occur in most tumors. The question therefore arises as to whether its overexpression in the other nephroblastomas is driven by LTR sequences acting as constitutive enhancers (36) which are located several tens of kilobases upstream or downstream of *nov*. In this respect, it is important to recall that in all tumors except 725, the *nov* transcripts are similar in apparent size to that expressed in normal cells.

The expression of *nov* is probably not transforming per se in all tissues, since large amounts of *nov* transcripts were detected in normal adult brain and lung. Also, the expression of *nov* cannot be definitely correlated with a particular stage of differentiation, because (i) both adult and embryonic brain cells, and adult lung cells, contain large amounts of *nov* transcripts and (ii) a significant level of *nov* is expressed only in embryonic kidney cells. Also, the expression of *nov* is not simply dependent on either proviral infection or active multiplication of transformed cells, because *nov* transcripts were not detectable in pretumoral kidneys or in tumorigenic BM2 and MSB1 chicken cell lines.

The use of recombinant replication-competent retroviral constructs expressing either the intact or the truncated *nov* gene demonstrated that the expression of the amino-terminal-truncated *nov* gene was sufficient to induce cellular transformation of CEF and that the overexpression of the normal gene had an inhibitory effect on the multiplication of the same cells. The lack of a suitable system, such as blastema cells, has not allowed us to test the biological role of *nov* on kidney cells in vitro.

Our observations have established the oncogenic potential of the truncated *nov* polypeptide and indicate that the

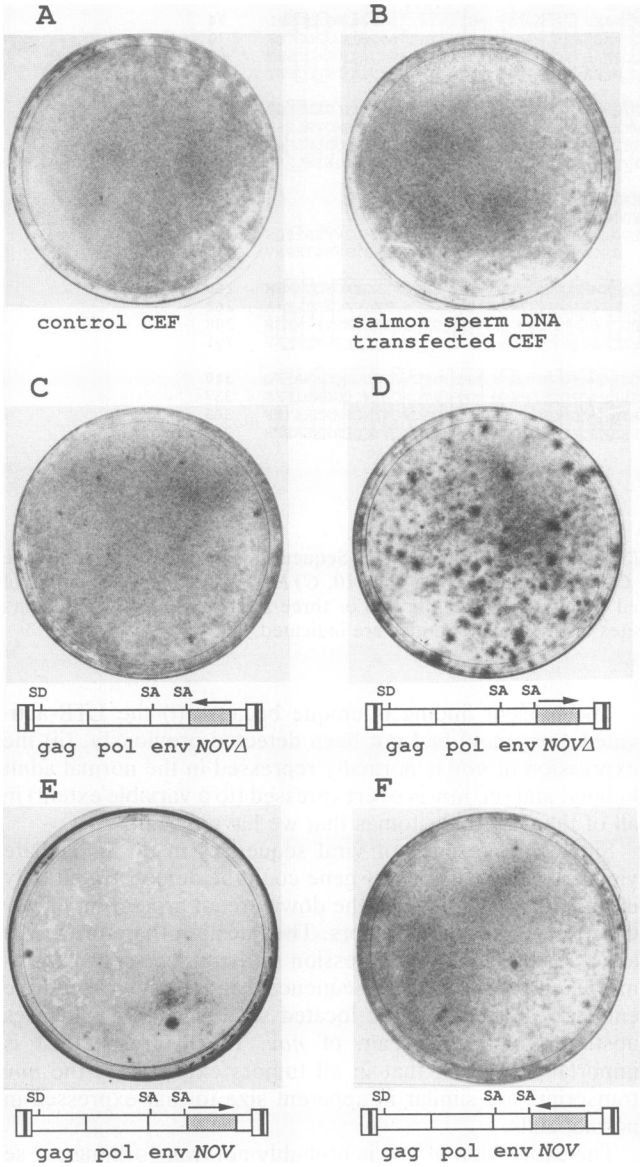

FIG. 6. Transformation of CEF induced by a truncated *nov*. Secondary CEF (A) were transfected with DNA from salmon sperm (B), pRSV 170 (C), pRSV 171 (D), pRSV 172 (E), or pRSV 173 (F). Structures of the recombinant clones are described in Materials and Methods. Plates were stained with Giemsa stain 13 days posttransfection. The average numbers of transformed cells foci per 10^6 cells calculated from duplicate dishes were 0 (A), 0 (B), 1.4 (C), 13.5 (D), 0.8 (E), and 1.4 (F).

biological effect of the normal *nov* product is different in fibroblastic and kidney cells. The possibility also exists that in addition to its putative IGF-binding activity, the *nov* protein possesses an unidentified biological function located in the conserved carboxy-proximal domain and that in kidney cells, transformation results from the overexpression of this function. Fibroblastic cells which already express *nov* would not respond in the same way to the overproduction of an intact *nov* polypeptide containing the carboxy-proximal domain and having the capacity to bind IGF. In this connection, it will be interesting to determine whether the truncated *nov* polypeptide which is overexpressed in tumor 725 is still able to bind IGF.

Interestingly, IGF II has been found to be overexpressed in some Wilms' tumors, and it has been proposed that it may be involved in tumor genesis (39, 44). Experiments are now in progress to determine whether expression of the *nov* sequences which are conserved in humans (30) is also upregulated in these tumors and whether *nov*-IGF interactions constitute a critical factor in the tumor process.

ACKNOWLEDGMENTS

V. Joliot (Maloisel) was the recipient of a fellowship from Association pour la Recherche contre le Cancer (ARC). This research was supported by grants from ARC, Institut National pour la Recherche Médicale (INSERM contract 900110), and Ligue Nationale Contre le Cancer.

We thank M. Marx for providing the fetal brain RNA preparation and S. H. Hughes for providing the RCAS and CLA12 vectors. We are grateful to M. Baluda (UCLA) and M. Center (KSU) for editing the manuscript. We also thank E. Moustacchi and J. Soret for critical reading of the manuscript and I. Gaspard and C. Pouget for photographic work.

ADDENDUM IN PROOF

Another polypeptide sharing 52% homology with *nov* has been described recently (CTGF; D. M. Bradham, A. Igarashi, R. L. Potter, and G. R. Grotendorst, J. Cell Biol. **114**:1285–1294, 1991). This protein has mitogenic and chemotactic properties and is the human homolog of *FISP-12*.

REFERENCES

1. **Albiston, A. L., and A. C. Herington.** 1990. Cloning and characterization of the growth hormone-dependent insulin-like growth factor binding protein (IGFBP-3) in the rat. Biochem. Biophys. Res. Commun. **166**:892–897.
2. **Alonso, S., A. Minty, Y. Bourlet, and M. E. Buckingham.** 1986. Comparison of β-actin coding sequences in the mouse: evolutionary relationships between the actin genes of warm blooded vertebrates. J. Mol. Evol. **23**:11–12.
3. **Beard, J. W., J.-F. Chabot, D. Beard, U. Heine, and G. E. Houts.** 1976. Renal neoplastic response to leukosis virus strain BAI A (avian myeloblastosis virus) and MC29. Cancer Res. **36**:339–353.
4. **Binkert, C., J. Landwehr, J.-L. Mary, J. Schwander, and G. Heinrich.** 1989. Cloning, sequence analysis and expression of a cDNA encoding a novel insulin-like growth factor binding protein (IGFBP-2). EMBO J. **8**:2497–2502.
5. **Boni-Schnetzler, M., J. Boni, F.-J. Ferdinand, and R. M. Franklin.** 1985. Developmental and molecular aspects of nephroblastomas induced by avian myeloblastosis-associated virus 2-0. J. Virol. **55**:213–222.
6. **Brinkman, A., C. Groffen, D. J. Kortleve, A. Geurts, A. G. van Kessel, and S. L. S. Drop.** 1988. Isolation and characterization of a cDNA encoding the low molecular weight insulin-like growth factor binding protein (IBP-1). EMBO J. **7**:2417–2423.
7. **Call, K. M., T. Glaser, C. Y. Ito, A. J. Buckler, J. Pelletier, D. A. Haber, E. A. Rose, A. Kral, H. Yeger, W. H. Lewis, C. Jones, and D. E. Housman.** 1990. Isolation and characterization of a zinc finger polypeptide gene at the human chromosome 11 Wilms' tumor locus. Cell **60**:509–520.
8. **Collart, K. L., R. Aurigemma, R. E. Smith, S. Kawai, and H. L. Robinson.** 1990. Infrequent involvement of c-*fos* in avian leukosis virus-induced nephroblastoma. J. Virol. **64**:3541–3544.
9. **Dunnill, M. S.** 1984. Pathological basis of renal disease, 2nd ed. Baillière Tindall, London.
10. **Eisenberg, D., E. Schwarz, M. Komaromy, and R. Wall.** 1984. Analysis of membrane and surface protein sequences with the hydrophobic moment plot. J. Mol. Biol. **179**:125–142.
11. **Fearon, E. R., B. Vogelstein, and A. P. Feinberg.** 1984. Somatic deletion and duplication of genes on chromosome 11 in Wilms'

tumours. Nature (London) **309**:176–178.
12. **Flyer, D. C., S. J. Burakoff, and D. V. Faller.** 1983. Cytotoxic T lymphocyte recognition of transfected cells expressing a cloned retroviral gene. Nature (London) **305**:815–818.
13. **Gessler, M., A. Poustka, W. Cavenee, R. L. Neve, S. H. Orkin, and G. A. P. Bruns.** 1990. Homozygous deletion in Wilms tumours of a zinc-finger gene identified by chromosome jumping. Nature (London) **343**:774–778.
14. **Goodenow, M. M., and W. S. Hayward.** 1987. 5′ long terminal repeats of *myc*-associated proviruses appear structurally intact but are functionally impaired in tumors induced by avian leukosis viruses. J. Virol. **61**:2489–2498.
15. **Grossberger, D.** 1987. Minipreps of DNA from bacteriophage lambda. Nucleic Acids Res. **15**:6737.
16. **Grundy, P., A. Koufos, K. Morgan, F. P. Li, A. T. Meadows, and W. K. Cavenee.** 1988. Familial predisposition to Wilms' tumour does not map to the short arm of chromosome 11. Nature (London) **336**:374–376.
17. **Guillon, J.-C., I. Chouroulinkov, and L. Renault.** 1963. Les tumeurs rénales spontanées des gallinacés. A propos de 23 observations. Bull. Cancer **50**:593–620.
18. **Heine, U., G. De Thé, H. Ishiguro, J. R. Sommer, D. Beard, and J. W. Beard.** 1962. Multiplicity of cell response to the BAI strain A (myeloblastosis) avian tumor virus. II. Nephroblastoma (Wilms' tumor): ultrastructure. J. Natl. Cancer Inst. **29**:41–61.
19. **Helmboldt, C. F., and B. S. Jorttner.** 1966. Histologic patterns of the avian embryonal nephroma. Avian Dis. **10**:452–462.
20. **Holt, C. A., K. Osorio, and F. Lilly.** 1986. Friend virus-specific cytotoxic T lymphocytes recognize both *gag* and *env* gene-coded specificities. J. Exp. Med. **164**:211–226.
21. **Huff, V., D. A. Compton, L.-Y. Chao, L. C. Strong, C. F. Geiser, and G. F. Saunders.** 1988. Lack of linkage of familial Wilms' tumour to chromosomal band 11p13. Nature (London) **336**:377–378.
22. **Hughes, S. H., J. J. Greenhouse, C. J. Petropoulos, and P. Sutrave.** 1987. Adaptor plasmids simplify the insertion of foreign DNA into helper-independent retroviral vectors. J. Virol. **61**: 3004–3012.
23. **Ishiguro, H., D. Beard, J. R. Sommer, U. Heine, G. De Thé, and J. W. Beard.** 1962. Multiplicity of cell response to the BAI strain A (myeloblastosis) avian tumor virus. I. Nephroblastoma (Wilms' tumor): gross and microscopic pathology. J. Natl. Cancer Inst. **29**:1–38.
24. **Jones, D. B.** 1957. Nephrotic glomerulonephritis. Am. J. Pathol. **33**:313–329.
25. **Kiefer, M. C., R. S. Ioh, D. M. Bauer, and J. Zapf.** 1991. Molecular cloning of a new human insulin-like growth factor binding protein. Biochem. Biophys. Res. Commun. **176**:219–225.
26. **Koufos, A., P. Grundy, K. Morgan, K. A. Aleck, T. Hadro, B. C. Lampkin, A. Kalbakji, and W. K. Cavenee.** 1989. Familial Wiedemann-Beckwith syndrome and a second Wilms tumor locus both map to 11p15.5. Am. J. Hum. Genet. **44**:711–719.
27. **Koufos, A., M. F. Hansen, B. C. Lampkin, M. L. Workman, N. G. Copeland, N. A. Jenkins, and W. K. Cavenee.** 1984. Loss of alleles at loci on human chromosome 11 during genesis of Wilms' tumour. Nature (London) **309**:170–172.
28. **Maloisel, V., and B. Perbal.** 1989. Efficiency of commercial in vitro packaging extracts, p. 508. *In* A practical guide to molecular cloning. John Wiley & Sons Inc., New York.
29. **Maloisel, V., and B. Perbal.** 1990. Why not use dichloromethane instead of noxious chloroform for nucleic acids extractions? Methods Mol. Cell. Biol. **1**:245–247.
30. **Martinerie, C., and B. Perbal.** 1991. Expression of a gene encoding a novel potential IGF binding protein in human tissues. C.R. Acad. Sci. (Paris) **313**:345–351.
31. **Nishizawa, M., N. Goto, and S. Kawai.** 1987. An avian transforming retrovirus isolated from a nephroblastoma that carries the *fos* gene as the oncogene. J. Virol. **61**:3733–3740.
32. **O'Brien, T. P., G. P. Yang, L. Sanders, and L. F. Lau.** 1990. Expression of *cyr-61*, a growth factor-inducible immediate-early gene. Mol. Cell. Biol. **10**:3569–3577.
33. **Orkin, S. H., D. S. Goldman, and S. E. Sallan.** 1984. Development of homozygosity for chromosome 11p markers in Wilms' tumour. Nature (London) **309**:172–174.
34. **Perbal, B.** 1988. A practical guide to molecular cloning. John Wiley & Sons Inc., New York.
35. **Perbal, B., J. S. Lipsick, J. Svoboda, R. F. Silva, and M. A. Baluda.** 1985. Biologically active proviral clone of myeloblastosis-associated virus type 1: implications for the genesis of avian myeloblastosis virus. J. Virol. **56**:240–244.
36. **Peters, G.** 1990. Oncogenes at viral integration sites. Cell Growth Differ. **1**:503–510.
37. **Ping, A. J., A. E. Reeve, D. J. Law, M. R. Young, M. Boehnke, and A. P. Feinberg.** 1989. Genetic linkage of Beckwith-Wiedemann syndrome to 11p15. Am. J. Hum. Genet. **44**:720–723.
38. **Plata, F., P. Langlade-Demoyen, J. P. Abastado, T. Berbar, and P. Kourilsky.** 1987. Retrovirus antigens recognized by cytolytic T lymphocytes activate tumor rejection *in vivo*. Cell **48**:231–240.
39. **Reeve, A. E., M. R. Eccles, R. J. Wilkins, G. I. Bell, and L. J. Millow.** 1985. Expression of insulin-like growth factor-II transcripts in Wilms' tumour. Nature (London) **317**:258–260.
40. **Reeve, A. E., P. J. Housiaux, R. J. M. Gardner, W. E. Chewings, R. M. Grindley, and L. J. Millow.** 1984. Loss of a Harvey *ras* allele in sporadic Wilms' tumour. Nature (London) **309**:174–176.
41. **Ryseck, R.-P., H. Macdonald-Bravo, M.-G. Mattéi, and R. Bravo.** 1991. Structure, mapping, and expression of *fisp-12*, a growth factor-inducible gene encoding a secreted cysteine-rich protein. Cell Growth Differ. **2**:225–233.
42. **Sanger, F., S. Nicklen, and A. R. Coulson.** 1977. DNA sequencing with chain-terminating inhibitors. Proc. Natl. Acad. Sci. USA **74**:5463–5467.
43. **Schwartz, C. E., D. A. Haber, V. P. Stanton, L. C. Strong, M. H. Skolnick, and D. E. Housman.** 1991. Familial predisposition to Wilms tumor does not segregate with the WT1 gene. Genomics **10**:927–930.
44. **Scott, J., J. Cowell, M. E. Robertson, L. M. Priestley, R. Wadey, B. Hopkins, J. Pritchard, G. I. Bell, L. B. Rall, C. F. Graham, and T. J. Knott.** 1985. Insulin-like growth factor-II gene expression in Wilms' tumour and embryonic tissues. Nature (London) **317**:260–262.
45. **Shaw, G., and R. Kamen.** 1986. A conserved AU sequence from the 3′ untranslated region of GM-CSF mRNA mediates selective mRNA degradation. Cell **46**:659–667.
46. **Siller, W. G.** 1981. Renal pathology of the fowl: a review. Avian Pathol. **10**:186–262.
47. **Simmons, D. L., D. B. Levy, Y. Yannoni, and R. L. Erikson.** 1989. Identification of a phorbol ester-repressible v-*src*-inducible gene. Proc. Natl. Acad. Sci. USA **86**:1178–1182.
48. **Smith, R. E., and C. Moscovici.** 1969. The oncogenic effects of nontransforming viruses from avian myeloblastosis virus. Cancer Res. **29**:1356–1366.
49. **Soret, J., G. Dambrine, and B. Perbal.** 1989. Induction of nephroblastoma by myeloblastosis-associated virus type 1: state of proviral DNAs in tumor cells. J. Virol. **63**:1803–1807.
50. **Soret, J., C. Krycève-Martinerie, J. Crochet, and B. Perbal.** 1985. Transformation of Brown Leghorn chicken embryo fibroblasts by avian myeloblastosis virus. J. Virol. **55**:193–205.
51. **Vogt, P. K.** 1969. Focus assay of Rous sarcoma virus, p. 198–211. *In* K. Habel and N. P. Salzman (ed.), Fundamental techniques in virology. Academic Press, Inc., New York.
52. **von Heijne, G.** 1983. Patterns of amino acids near signal-sequence cleavage sites. Eur. J. Biochem. **133**:17–21.
53. **Watts, S. L., and R. E. Smith.** 1980. Pathology of chickens infected with avian nephroblastoma virus MAV-2(N). Infect. Immun. **27**:501–512.
54. **Watts, S. L., R. E. Smith, and A. J. Faras.** 1982. Avian nephroblastoma virus MAV-2(N) and avian osteopetrosis virus MAV-2(O) are genetically distinct. J. Gen. Virol. **60**:185–189.
55. **Westaway, D., J. Papkoff, C. Moscovici, and H. E. Varmus.** 1986. Identification of a provirally activated c-Ha-*ras* oncogene in an avian nephroblastoma via a novel procedure: cDNA cloning of a chimaeric viral-host transcript. EMBO J. **5**:301–309.